# A Novel Model of Solute Transport in a Hollow-Fiber Bioartificial Pancreas Based on a Finite Element Method

**Jean-Luc Dulong,[1] Cécile Legallais,[1] Sylviane Darquy,[2] Gérard Reach[2]**

*[1]Laboratoire de Biomecanique et Génie Biomédical, Université de Technologie de Compiègne, UMR 6600 CNRS, BP20529, 60205 Compiègne, France; telephone: +33 3 44 23 44 01; fax: +33 3 44 20 48 13; email: cecile.legallais@utc.fr*
*[2]INSERM Unité 341, Department of Diabetology, Hôtel-Dieu Hospital, Paris, France*

*Received 4 September 2001; accepted 7 December 2001*

*DOI: 10.1002/bit.10230*

**Abstract**: Extravascular bioartificial pancreas based on hollow fiber seems to be a promising treatment of diabetes mellitus. However, solutes mass-transport limitations in such a device could explain its lack of success. To determine critical device parameters, we have developed a novel tridimensional model based on finite element method for glucose, insulin, and oxygen diffusion around an islet of Langerhans encapsulated in a hollow-fiber section. A glucose ramp stimulation was applied outside the fiber and diffused to the islet. Concomitantly, a stationary oxygen partial pressure was applied outside the fiber, and determined local oxygen partial pressure on the islet environment. An insulin secretion model stimulated by a glucose concentration ramp and corrected by the local oxygen partial pressure was also implemented. Insulin secretion by the islet was thus computed as a response to glucose signal. The model predictions notably showed that the fiber radius had to be small enough to favor a fast response for insulin secretion and to ensure a maximal oxygen partial pressure in the islet environment. Besides the effect of fiber radius, a better islet oxygenation could be achieved by adjustments on the islet density, i.e., on the fiber length dedicated to a single islet. These hints should allow the future proposal of an optimal design for an implantable bioartificial pancreas.  *Biotechnol Bioeng* **78:** 576–582, 2002.
**Keywords**: bioartificial pancreas; mass transfer; hollow fiber; finite element; islet density

## INTRODUCTION

Currently, pancreas and islet transplantation for the treatment of type 1 diabetes is limited by the need for an immunosuppressive treatment aimed to prevent the rejection of transplanted tissue. The recent breakthrough by Shapiro et al. (2000), of successful islet transplantation demonstrates that islets transplanted in the liver of diabetic patients can completely correct diabetes for more than one year. However, the dangers of the new immunosuppressive regimen proposed by the Edmonton team remain unknown. For this reason, the implantable bioartificial pancreas based on pancreatic tissue immunoprotected by a permselective membrane represents an attractive alternative.

Several shapes of extravascular bioartificial pancreas implanted subcutaneously or in the peritoneal cavity have been studied. Compared to microencapsulation in beads (Calafiore et al., 1999; De Vos et al., 1993; Duvivier-Kali et al., 2001; Hunkeler, 1999; Siebers et al., 1999; Soon-Shiong, 1999; Sun, 1997) hollow fibers (Delaunay et al., 1997; Hou and Bae, 1999; Lacy et al., 1991;) and diffusion chambers (Rafael et al., 1997) were easy to retrieve after their implantation. However, performances of such devices were extremely variable (Colton and Avgoustiniatos, 1991).

In a bioartificial pancreas, islets of Langerhans viability and functions should be maintained on a long term basis. This requires an appropriate supply of nutriments and oxygen. In response to glucose stimulation, insulin release in blood should be fast enough to ensure an efficient regulation. Unfortunately, the extravascular implantation results in poor diffusive exchanges between the islets and the surrounding blood. In addition, oxygen local partial pressure is low in the peritoneal cavity (40 mmHg). It affects insulin secretion (Dionne et al., 1993); yet islet necrosis frequently occurs at the center of the fiber (Colton, 1995; Lacy et al., 1991). For these reasons, a detailed analysis of the mass-transport limitation for the three species of interest: glucose, insulin, and oxygen is mandatory. Solutes diffusion models for an extravascular hollow-fiber bioartificial pancreas have already been published: they focussed either on glucose and insulin diffusion (Buladi et al., 1996; Young et al., 1998) or oxygen diffusion (Avgoustiniatos and Colton, 1997), but never on both aspects.

Here we describe a versatile model based on a finite element method developed to investigate various hol-

*Correspondence to:* Cécile Legallais
Contract grant sponsor: INSERM-CNRS
Contract grant number: Ingénierie tissulaire, 2000

low-fiber geometries. It takes into account the diffusion of the three mentioned solutes under physiologically relevant conditions. Our aim was to determine the parameters critical for the successful implantation of such a bioartificial organ.

## METHODS

### Geometry

The complete model aimed at describing the mass transfer of the three solutes (glucose, insulin, oxygen) around islets of Langerhans in a hollow fiber implanted in the peritoneal cavity. Within the fiber, the islets were encapsulated in a gel to adjust their density.

The first approach dealt with a single islet in a fiber section as presented in Figure 1. A sphere, modeling the islet, was located at the center of a cylinder representing the gel. The hollow-fiber membrane was not taken into account because the initial purpose was to optimize the geometry within the cylinder. Two geometrical parameters described the model: R, the internal radius of the hollow fiber and L, the half-length of the cylinder. The sphere diameter was set to 200 μm, i.e., the mean diameter of an islet of a rat.

The existing models and experiments, dealing with insulin secretion as a function of glucose (Jaffrin et al., 1988; Nomura et al., 1984) or of $P_{O_2}$ (Dionne et al., 1993), considered the islet as an entity, although it was an arrangement of individual cells. They did not discriminate cells near the surface from those at the center. In the absence of any reliable data, we had to describe the islet as a hollow sphere. The boundary conditions reflected the behavior already depicted in the literature.

### General Description of the Insulin Secretion Model

Insulin secreted out of the cylinder responded to external glucose stimulation and depended on the stationary surrounding partial pressure of oxygen ($P_{O_2}$). The calculation was divided into four steps:

1. Transient glucose diffusion: An increasing ramp of glucose concentration (from 0.8 g/L to 3.0 g/L in 20 min) was imposed on the cylinder outer surface, and a glucose consumption, i.e., a glucose flux, on the sphere surface. The result was a gradient of glucose concentration with time between the islet and the cylinder surface.
2. Stationary oxygen diffusion: A steady oxygen concentration was simultaneously imposed on the cylinder outer surface, and an oxygen consumption on the sphere surface. The usual oxygen concentration in the peritoneal cavity correspond to a $P_{O_2}$ of 40 mmHg, but here it could be lower due to the presence of a membrane around the cylinder. The result was a constant gradient of oxygen concentration between the islet and the cylinder surface.
3. Insulin secretion: The insulin flux secreted by the islet resulting from glucose concentration kinetics and steady oxygen concentration on the islet surface was calculated by an adapted model as described late.
4. Transient insulin back diffusion: The insulin flux secreted near the islet diffused back to the cylinder surface.

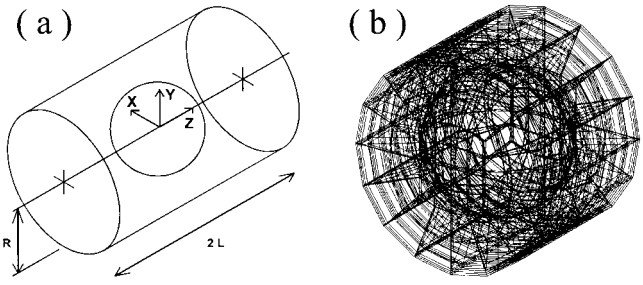


**Figure 1.** Geometric sketch of the spherical islet located at the center of an alginate gel cylinder (a), and the complete geometric mesh with HEX 8 elements (b).

### Conservation Equations

A finite element model was used to describe the three diffusion steps. Such a model easily allowed many geometric modifications.

The geometry meshing was realized with HEX 8 elements (hexahedrons with 8 degrees of freedom) by the commercial software Patran® (MacNeal-Schwendler Corporation, Los Angeles, CA) as shown in Figure 1. We used the associated calculation code software Nastran® (MacNeal-Schwendler Corporation) to solve the three diffusion steps. Initially, this software was able to solve only thermal diffusion problems. We adapted it to solve mass-diffusion equations thanks to the Reynolds analogy (Bird et al., 1960) by setting to one the density and the specific heat.

### Constitutive Equations

The solute diffusivities in a 2% alginate gel, at 37°C, ($D_{eff}$) were calculated with Mackie and Meares model (Riley et al., 1999; Westrin and Axelsson, 1991): $267.10^{-5}$ $mm^2/s$ for oxygen (Avgoustiniatos and Colton, 1997; Sridhar, 1983), $78.10^{-5}$ $mm^2/s$ for glucose (Axelsson and Persson, 1988; Morvan and Jaffrin, 1989), $18.10^{-5}$ $mm^2/s$ for insulin (Morvan and Jaffrin, 1989), respectively.

Glucose and oxygen consumptions by the islets depended on glucose and oxygen concentrations respectively, under Michaelis-Menten kinetics. However, in our model the variations were small enough to consider the consumptions constant as a first approximation: glucose consumption was set to $10^{-5}$ μg/s/islet (Buladi et al., 1996; Trus et al., 1981). For oxygen, two extreme values were found in the literature: $1.6.10^{-6}$ and $4.3.10^{-6}$ μg/s/islet

(Avgoustiniatos et Colton, 1997; Tziampazis and Sambanis, 1995) and implemented in the computation.

As already mentioned, insulin secretion was a function of both glucose concentration kinetics and oxygen concentration. In the absence of any model in the literature, a secretion model combining the effects of both solutes was elaborated. It was based on Jaffrin's R model (Jaffrin et al., 1988) already developed for insulin secretion in response to a change in glucose concentration G(t). The response to a glucose ramp might be divided into two phases. A first secretion peak came from the quick release of insulin stored in the islets, and a second plateau secretion was due to newly produced insulin.

We postulated a linear correction of normoxic secretion model $R$ to find the oxygen-corrected secretion model $\tilde{R}$, as shown in Eq. (1):

$$\tilde{R}(t) = aR(t) + b \tag{1}$$

$a$ and $b$ parameters have been defined from Dionne's results (Dionne et al., 1993) and depended on an oxygen-correction factor noted β described in Appendix A.

### Calculation steps

The corrected insulin secretion model was completed using Matlab® software (MathWorks, Natick, MA). During step 3, local oxygen concentration $(P_{O_2})_i$ and local glucose concentration kinetics $G_i(t)$ were extracted from the finite element model on each node i of the sphere surface. Then, local insulin flux secreted $(\tilde{R})_i$ on the same node i was calculated, according to the procedure described in Appendix B.

## RESULTS

To understand the effect of geometric parameters on the efficiency of the bioartificial pancreas, four different geometries were investigated. Two different R and L values were studied (Table I). Islet density was obviously different according to these geometries as shown in Figure 2.

Glucose and oxygen concentrations were shown on two nodes of interest: Node A was located on the cylinder axis (x = 0, y = 0, z = 0.10), and thus was the farthest from the cylinder; in contrast, node B (x = 0, y = 0.10, z = 0) was the closest node to the cylinder.

### Glucose Diffusion

A glucose stimulation ramp from 0.8 to 3.0 g/L was generated at the external cylinder surface. Glucose concentrations are shown in Figure 3 for each geometrical configuration and each node on the islet. No difference in concentration or time course was detectable between results on node A and on node B, showing that glucose diffusion was very fast at islet scale.

**Table I.** Dimensions of the four different geometric models.

| Model name | lr | Lr | lR | LR |
|---|---|---|---|---|
| Cylinder length L (mm) | 0.15 | 1.00 | 0.15 | 1.00 |
| Internal radius R (mm) | 0.15 | 0.15 | 1.00 | 1.00 |

Glucose kinetics with the small radius geometry (r.l and r.L) was comparable to the external glucose stimulation. In contrast, with a large radius, a significant delay (5 min) appeared between cylinder and islet surface. Thus, glucose mass transfer through alginate was mostly dependent on the diffusion length, i.e., the cylinder radius. The role of cylinder length was negligible. No difference appeared between short or long cylinder, showing that glucose diffusion was mainly radial.

### Oxygen Diffusion

Under different conditions described in Methods, a static oxygen partial pressure gradient was obtained as shown in Figure 4. Oxygen partial pressure was the highest on node B of the islet surface, and the lowest on node A. The presence of the islet at the cylinder center strongly affected the oxygen profile. Significant oxygen gradients were observed, resulting from a very low $P_{O_2}$ at the islet surface due to significant oxygen consumption. In addition, the $P_{O_2}$ was submitted to the islet influence even far from its surface, especially on the cylinder axis.

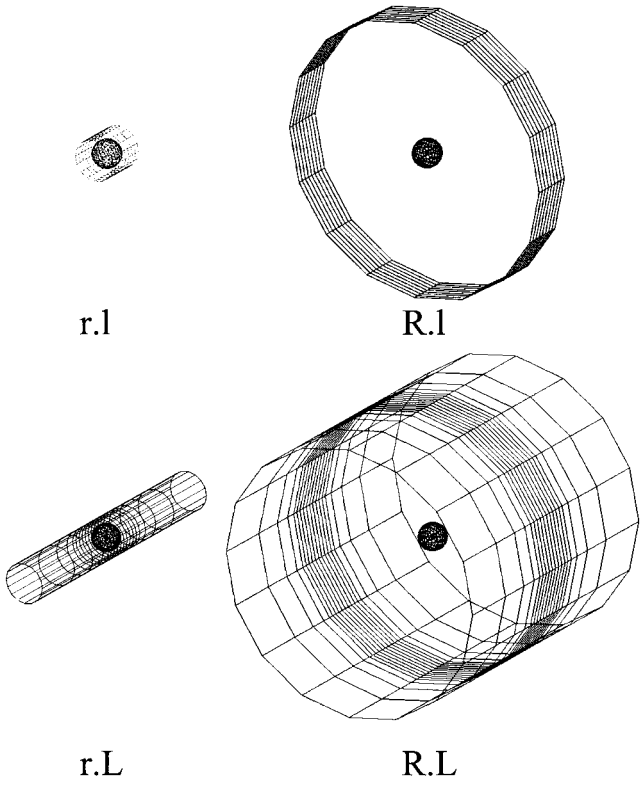


**Figure 2.** Finite element geometries studied.

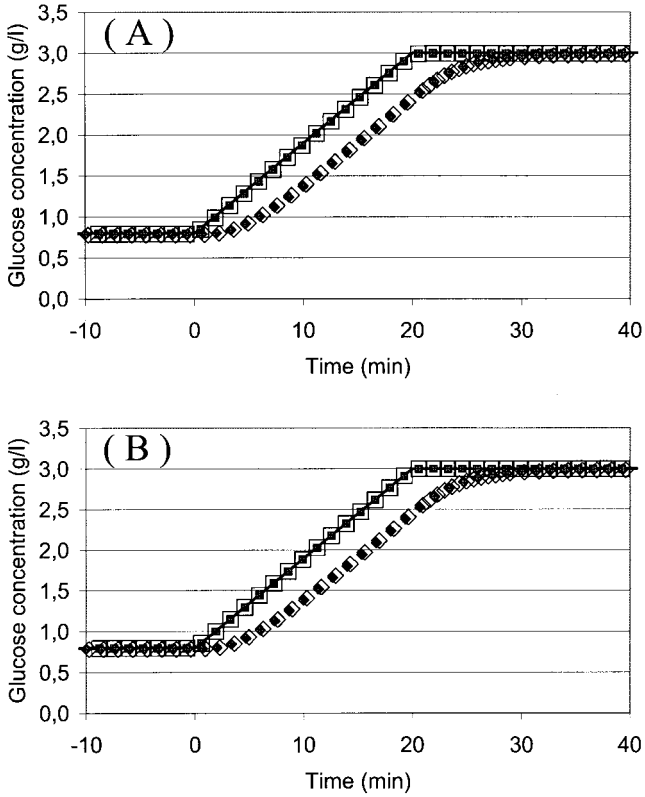


**Figure 3.** Different glucose concentration kinetics in the four geometric models [(□) r.l model, (■) r.L model, (◇) R.l model, (◆) R.L model], on node A or B, with a glucose stimulation from 0.8 g/L to 3.0 g/L in 20 min on the cylinder surface.

Figure 5 shows the constant oxygen local partial pressure on both islet selected nodes, for an external $P_{O_2}$ of 40 mmHg, for the same geometric models. This case was representative of all the other pressure cases. Indeed, two boundary conditions affected the $P_{O_2}$ profile in alginate. On the one hand, oxygen consumption imposed the oxygen gradient shape, while on the other hand, external oxygen partial pressure determined the partial pressure origin. Other external partial pressure cases were thus deducted by a simple partial pressure shift.

It should be noted that whatever the case studied, the $P_{O_2}$ on the islet was always lower than that at the cylinder surface. As for glucose, the most significant geometric effect was that of radius—a large radius resulted in a low $P_{O_2}$ on the islet. This effect could be counterbalanced by a sufficient cylinder length. In this case, islet oxygen supply could be ensured also by oxygen present along the cylinder axis, and not only at the cylinder periphery.

In fact, oxygen on the islet mainly depended on its consumption. In the case of high consumption, only a small diffusion length from the periphery could offer a correct $P_{O_2}$ on the islet, although it was almost divided by two on node A compared to the external value. In the most critical cases, $P_{O_2}$ was very close to zero, leading to potential necrosis.

The second aspect of oxygen pressure study was its effect on insulin secretion by the islet. The mean oxygen-correction factor $\bar{\beta}$ defined by Eq. (2) at the sphere surface nodes indicated how the second phase secretion was reduced in the bioartificial pancreas (see appendices for notations).

$$\bar{\beta} = \frac{1}{n}\sum_{i=1}^{n} \beta_i \tag{2}$$

Results on $\bar{\beta}$ are shown in Figure 6, for the four geometric models, the same three external partial pressure cases and both extreme oxygen consumptions. Because $\beta$ did not linearly vary according to $P_{O_2}$, $\bar{\beta}$ highlighted the differences between low and high $P_{O_2}$ on the islet.

Under physiological conditions (140 mmHg), encapsulation was not deleterious. Insulin mass secreted would be maximal. Under a low external oxygen partial pressure (20 mmHg), $\bar{\beta}$ was very low (<20%) and necrosis was expected in half of the cases. Under peritoneal oxygen conditions, some satisfying results ($\bar{\beta} > 40\%$)

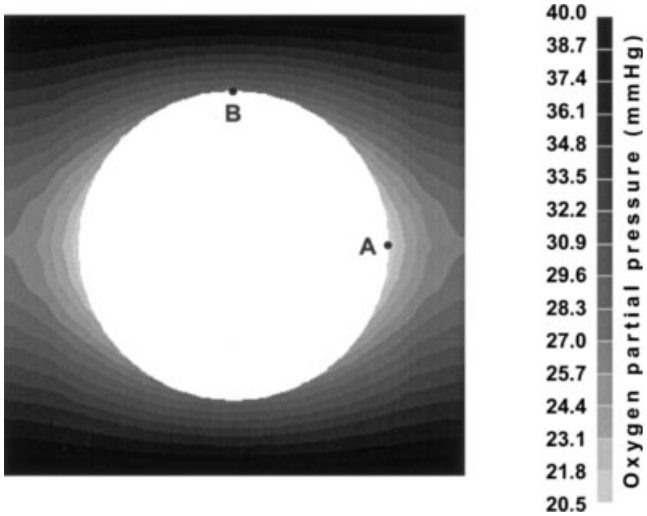


**Figure 4.** Oxygen concentration field, in a (Y,Z) plane, with the r.l geometric model, under high oxygen consumption and external oxygen partial pressure of 40 mmHg.

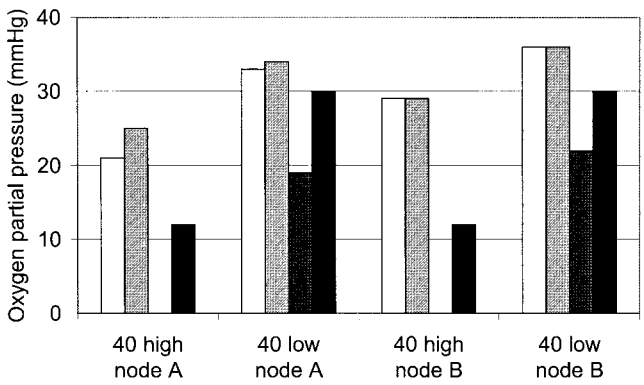


**Figure 5.** Node A and node B oxygen partial pressures as a function of geometric model [(□) r.l model; (■) r.L model, (■) R.l model, (■) R.L model), oxygen consumption (low or high). External oxygen concentration was 40 mmHg.

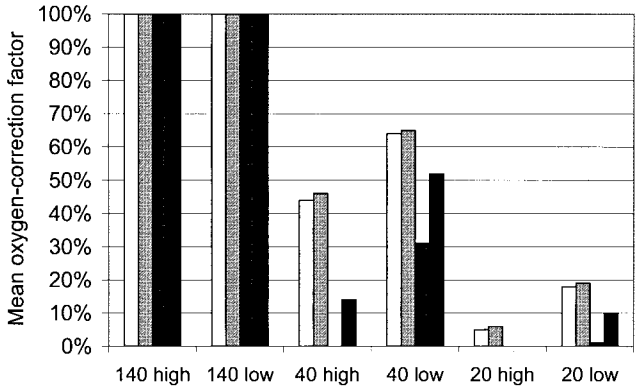


**Figure 6.** Mean oxygen-correction factor $\bar{\beta}$ as a function of geometric model [(□) r.l model; (▩) r.L model, (■) R.l model, (■) R.L model), oxygen consumption (low or high) and external oxygen concentration (140, 40, or 20 mmHg).

could be obtained. High oxygen consumption dramatically reduced $\bar{\beta}$ results when radius was large or cylinder length short. It was interesting to note that an adequate oxygen-correction factor can be obtained (52%) with low oxygen consumption and large radius provided that cylinder length was long enough.

## Insulin Back Diffusion

The results of step 4 dealing with insulin secretion out of the cylinder are shown in Figure 7 for the 40 mmHg external oxygen case. Insulin secretions for the four geometric models were compared to the insulin secretion of a nonencapsulated islet. In fact, the case R.l could not be computed with high oxygen consumption because islet necrosis was suspected.

Even when a small radius was employed, the insulin secretion was much lower than that of a nonencapsulated islet. Time response essentially depended on the cylinder radius. It could be much too long (30 min) with a large radius. Moreover, cylinder length influence on time response was totally negligible. On the contrary, amplitude response was, as the mean oxygen-correction factor $\bar{\beta}$, affected by all the parameters considered, notably cylinder length. The most significant effect was observed for a large radius, where the secretion peak disappeared and second-phase amplitude was much lower than in the small radius case.

## DISCUSSION

The above results obtained from a novel model for insulin secretion based on the finite element method permitted the evaluation of the influence of fiber geometry. Such a versatile method solved the three dimension diffusion problem and easily accounted for the geometry variations.

Glucose kinetics on islet surface was comparable to a ramp kinetics, in every case. The use of Jaffrin's model

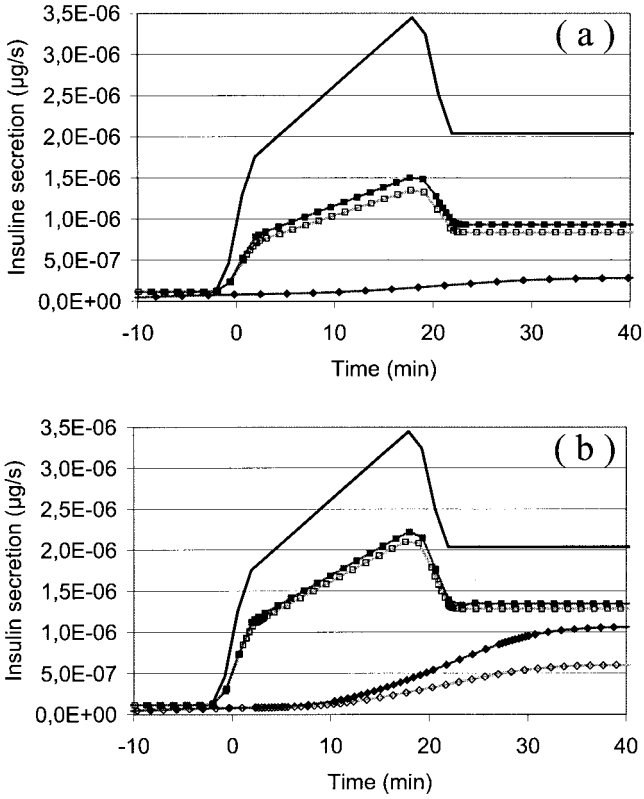


**Figure 7.** Insulin secretion for an islet alone or out of the cylinder (islet in the bioartificial pancreas) for each four geometric models [(□) r.l model; (■) r.L model, (◇) R.l model, (◆) R.L model] with high (a) or low (b) oxygen consumption.

was thus correct for the insulin secretion calculation step. In fact, the time response for glucose diffusion from the periphery to the islet was only affected by the cylinder radius.

Each geometric parameter (radius and length), and each physiological parameter (external partial pressure and consumption by islet), were influent on oxygen supply to islet. This suggested that the geometric parameters, notably the islet density, could be optimized. However, a better knowledge on the physiological parameters would be necessary to improve the simulation of the oxygen supply. It was not possible to precisely conclude on islet necrosis due to the lack of diffusion data inside the islet. It is well-known that necrotic region occurs first in the center of islets. Hence, with a low $P_{O_2}$ on islet surface, a necrotic region was likely to appear and so to reduce the amount of islet tissue able to secrete insulin. Moreover, the oxygen-correction factor $\beta$ did not take into account necrosis inside the islet. Indeed, to measure it, Dionne et al. (1993) decreased the $P_{O_2}$ during a short time, and necrosis could not occur. In the long run, the necrosis appearance would increase the effect of oxygen.

Although insulin secretion certainly depended on other physiological signals, oxygen and glucose concentrations were supposed to be preponderant. There-

fore, insulin secretions main features could be deducted from glucose and oxygen conclusions—a large radius increased time response and reduced second phase amplitude. Moreover, a large radius was shown to eliminate the first-phase secretion peak. This would induce poor insulin kinetics and thus a low quality of the glycemia regulation. Incidentally, this effect of increasing the distance between the outer membrane and the islets has been observed experimentally with microencapsulated rat islets (Chicheportiche and Reach, 1988). By contrast, increasing the cylinder length, and thus decreasing the islet density, allowed the enhancement of the second-phase amplitude.

Colton, following Dionne's results on the effect of local $P_{O_2}$ on insulin secretion, already showed with a one dimension model that cylinder radius should be minimal (Avgoustiniatos and Colton, 1997). However, our model indicated that a larger radius geometry could be similar to that of low radius, provided that oxygen consumption was low and cylinder length was significant, i.e., that islet density was low. In this configuration, oxygen consumption would be high enough to generate a longitudinal diffusion in the cylinder. With an adequate cylinder length (i.e., with an islet density low enough), oxygen supply could be correctly achieved by using the additional membrane surface devoted to a single islet. A total necrosis could be avoided (Fig. 5), while a correct secretion factor of 30 to 50% could be obtained with a 40 mmHg external oxygen partial pressure, and with a low oxygen consumption (Fig. 6). In this case, the large internal dead volume in the hollow fiber would not lead to insulin dilution because cylinder length was shown to be influent neither on the first peak nor on the second phase of insulin response time (Fig. 7). This result was different from that found in a vascular bioartificial pancreas (Jaffrin et al., 1988). Only a short diffusion length had to be ensured to avoid insulin dilution. This point was important and allowed the decrease of islet density.

Taken together, these considerations indicated that fiber geometry could be optimized; radius should be minimal to reduce diffusion length and time response. Moreover, islet density should be low enough to enhance islet oxygenation. However, with a low islet density, the problem would be to obtain a device small enough to be implanted and containing an adequate number of islets. This model may therefore be useful to find a compromise between the ultimate size of the device and its functions. An optimization of the islet density could be considered in a future study.

## CONCLUSIONS

Our model of insulin secretion was the first taking into account multiple solute diffusion. Results presented here showed that the optimization of the hollow-fiber geometry (radius and islet density) should maximize insulin secretion in a bioartificial implantable pancreas.

Interestingly, most of the bioartificial pancreas developed in the past contained a gel. This gel might not only immobilize the islets, improving their viability, but also achieve islets spreading, according to our findings. Indeed, the reduction of islet density allowed the enhancement of oxygen supply to islets, and an optimal insulin secretion. However, it would increase implantable volume and might lead to unrealistic designs.

Decreasing the cylinder radius was thus not the only solution to maximize this oxygen supply, although it ensured a better profile and an acceptable time response for insulin secretion.

In conclusion, the implantation of an hollow-fiber bioartificial pancreas in the peritoneal cavity appears to be very delicate. Lack of islet density optimization could explain the poor in vivo results observed until now. Furthermore, local oxygen partial pressure was low and with a membrane, external oxygen partial pressure between 20 and 40 mmHg should be considered. For this reason, membranes inducing angiogenesis could offer new solutions to this problem.

Professor M. Y. Jaffrin is gratefully acknowledged for his helpful comments on this manuscript.

## APPENDIX A

In hypoxia ($P_{O_2} < 60$ mmHg), Dionne et al. (1993) quantified the fraction of normoxic second-phase insulin secretion as a function of bulk perfusate $P_{O_2}$. We called this fraction the oxygen-correction factor, noted β. Its value was given by Eq. (3).

$$\begin{cases} \beta = -8.3\times10^{-6}(P_{O_2})^3 + 7.1\times10^{-4}(P_{O_2})^2 + 3.7\times10^{-3}(P_{O_2}) \\ \qquad\qquad \text{if } (P_{O_2}) \le 60\,\text{mmHg} \\ \beta = 1 \\ \qquad\qquad \text{if } (P_{O_2}) > 60\,\text{mmHg} \end{cases} \tag{3}$$

Under conditions of hypoxia, basal secretion remained unchanged [Eq. (4)] but the second plateau phase was decreased by the oxygen-correction factor [Eq. (5)].

$$\tilde{R}(t=0) = R(t=0) \tag{4}$$

$$\tilde{R}(t=\infty) = \beta\ R(t=\infty) \tag{5}$$

Solving Eqs. (1), (4) and (5) gave the following solution for $a$ and $b$ :

$$\begin{cases} a = \frac{\beta R(\infty) - R(0)}{R(\infty) - R(0)} \\ b = (1-\beta)\frac{R(\infty)R(0)}{R(\infty) - R(0)} \end{cases} \tag{6}$$

Under severe hypoxia conditions, basal secretion decreased and was equal to the second plateau phase. [Eqs. (7) and (8)].

$$\tilde{R}(t=0) = \tilde{R}(t=\infty) \tag{7}$$

$$\tilde{R}(t=\infty) = \beta R(t=\infty) \tag{8}$$

In this case, where $R(0) > \beta R(\infty)$, solving Eqs. (1), (7), and (8) allowed to find $a$ and $b$:

$$\begin{cases} a = 0 \\ b = \beta R(\infty) \end{cases} \tag{9}$$

## APPENDIX B

On each node, the normoxic local secretion $(R)_i$ was first calculated as a function of local glucose concentration kinetics $G_i(t)$ by equation (10), $n$ being the total node number at the sphere surface.

$$(R)_i = \frac{R(G_i[t])}{n} \tag{10}$$

Then, each local oxygen-correction factor $\beta_i$ was calculated, on each node, knowing $(P_{O_2})_i$.

Hence, the local corrected insulin secretion model $(\tilde{R})_i$ was determined and calculated on each node as a function of $(R)_i$ and $\beta_i$ .

These nodal insulin secretions $(\tilde{R})_i$ were used as flux boundary conditions into finite element model during step 4 to calculate the insulin diffusion in alginate.

## References


Avgoustiniatos ES, Colton CK. 1997. Effect of external oxygen mass transfer resistances on viability of immunoisolated tissue. Ann NY Acad Sci 831:145–167.

Axelsson A, Persson B. 1988. Determination of effective diffusion coefficients in calcium alginate gel plates with varying yeast cell content. Appl Biochem Biotechnol 18:231–250.

Bird RB, Stewart WE, Lightfoot EN. 1960. Transport phenomena. New York: Wiley. 780 p.

Buladi BM, Chang CC, Belovich JM, Gatica JE. 1996. Transport phenomena and kinetics in an extravascular bioartificial pancreas. Am Inst Chem Eng J 42:2668–2682.

Calafiore R, Basta G, Luca G, Boselli C, Bufalari A, Bufalari A, Cassarani MP, Giustozzi GM, Brunetti P. 1999. Transplantation of pancreatic islets contained in minimal volume microcapsules in diabetic high mammalians. Ann NY Acad Sci 18:219–232.

Chicheportiche D, Reach G. 1988. In vitro kinetics of insulin release by microencapsulated rat islets: Effect of the size of the microcapsules. Diabetologia 31:54–57.

Colton CK, Avgoustiniatos ES. 1991. Bioengineering in development of the hybrid artificial pancreas. J Biomech Eng 113:152–170.

Colton CK. 1995. Implantable biohybrid artificial organs. Cell Transplant. 4:415–436.

De Vos P, Wolters GH, Fritschy WM, Van Schilfgaarde R. 1993. Obstacles in the application of microencapsulation in islet transplantation. Intl J Art Org 16:205–212.

Delaunay C, Honiger J, Darquy S, Capron F, Reach G. 1997. Bioartificial pancreas containing porcine islets of Langerhans implanted in low-dose streptozotocin-induced diabetic mice: Effect of encapsulation medium. Diabetes Metab 23:219–227.

Dionne KE, Colton CK, Yarmush ML. 1993. Effect of hypoxia on insulin secretion by isolated rat and canine islets of Langerhans. Diabetes 42:12–21.

Duvivier-Kali VF, Omer A, Parent RJ, O'Neil JJ, Weir GC. 2001. Complete protection of islets against allorejection and autoimmunity by a simple barium-alginate membrane. Diabetes 50:1698–1705.

Hou QP, Bae YH. 1999. Biohybrid artificial pancreas based on macrocapsule device. Adv Drug Del Rev 35:271–287.

Hunkeler D. 1999. Bioartificial organs transplanted from research to reality. Natl Biotechnol 17:335–336.

Jaffrin MY, Reach G, Notelet D. 1988. Analysis of ultrafiltration and mass transfer in a bioartificial pancreas. J Biomech Eng 110:1–10.

Lacy PE, Hegre OD, Gerasimidi-Vazeou A, Gentile FT, Dionne KE. 1991. Maintenance of normoglycemia in diabetic mice by subcutaneous xenografts of encapsulated islets. Science 254:1782–1784.

Morvan D, Jaffrin MY. 1989. Unsteady diffusion mass transfer in a microencapsulated islet of Langerhans for a bioartificial pancreas. Intl J Heat Mass Transfer 32:995–1006.

Nomura M, Shichiri M, Kawamori R, Yamasaki Y, Iwama N, Abe H. 1984. A mathematical insulin-secretion model and its validation in isolated rat pancreatic islets perifusion. Comp Biomed Res 17: 570–579.

Rafael E, Tibell A, Arner P. 1997. Microdialysis for in vivo evaluation of permeability of immunoisolation devices. Transpl Proc 29: 2134–2135.

Riley MR, Muzzio FJ, Reyes SC. 1999. Experimental and modeling studies of diffusion in immobilized cell systems. A review of recent literature and patents. Appl Biochem Biotechnol 80:151–188.

Shapiro AM, Lakey JR, Ryan EA, Korbutt GS, Toth E, Warnock GL, Kneteman NM, Rajotte RV. 2000. Islet transplantation in seven patients with type 1 diabetes mellitus using a glucocorticoid-free immunosuppressive regimen. N Engl J Med 343:230–238.

Siebers U, Horcher A, Brandhorst H, Brandhorst D, Hering B, Federlin K, Bretzel RG, Zekorn T. 1999. Analysis of the cellular reaction towards microencapsulated xenogeneic islets after intraperitoneal transplantation. J Mol Med 77:215–218.

Soon-Shiong P. 1999. Treatment of type I diabetes using encapsulated islets. Adv Drug Del Rev 35:259–270.

Sridhar T. 1983. Transport coefficients of liquids. In: Cheremisinoff NP, Gupta R, editors. Handbook of fluids in motion. Stoneham, MA: Butterworth. p 3–28.

Sun AM. 1997. Advantages of microencapsulation as an immunoprotection method in the transplantation of pancreatic islets. Ann Transplant 2:55–62.

Trus MD, Zawalich WS, Burch PT, Berner DK, Weill VA, Matschinsky FM. 1981. Regulation of glucose metabolism in pancreatic islets. Diabetes 30:911–922.

Tziampazis E, Sambanis A. 1995. Tissue engineering of a bioartificial pancreas: Modeling the cell environment and device function. Biotechnol Prog, 11:115–126.

Westrin BA, Axelsson A. 1991. Diffusion in gels containing immobilized cells: A critical review. Biotechnol Bioeng 38:439–446.

Young TH, Chuang WY, Yao NK, Chen LW. 1998. Use of a diffusion model for assessing the performance of poly(vinyl alcohol) bioartificial pancreases. J Biomed Mater Res 40:385–391.